

Soft Matter

Accepted Manuscript



This is an *Accepted Manuscript*, which has been through the Royal Society of Chemistry peer review process and has been accepted for publication.

Accepted Manuscripts are published online shortly after acceptance, before technical editing, formatting and proof reading. Using this free service, authors can make their results available to the community, in citable form, before we publish the edited article. We will replace this *Accepted Manuscript* with the edited and formatted *Advance Article* as soon as it is available.

You can find more information about *Accepted Manuscripts* in the [Information for Authors](#).

Please note that technical editing may introduce minor changes to the text and/or graphics, which may alter content. The journal's standard [Terms & Conditions](#) and the [Ethical guidelines](#) still apply. In no event shall the Royal Society of Chemistry be held responsible for any errors or omissions in this *Accepted Manuscript* or any consequences arising from the use of any information it contains.

ARTICLE

Formulation and preparation of stable cross-linked alginate-zinc nanoparticles in the presence of monovalent salt

Cite this: DOI: 10.1039/x0xx00000x

Received 00th January 2012,
Accepted 00th January 2012

DOI: 10.1039/x0xx00000x

www.rsc.org/

Sara Pistone*, Dafina Qoragllu, Gro Smistad and Marianne Hiorth

Polysaccharide-based nanoparticles can be formed, under the right conditions, when a counterion is added to a dilute polysaccharide solution. In this study, the possibility of preparing stable alginate nanoparticles cross-linked with the cation zinc was investigated. The effects of the ionic strength of the solvent and of the concentration of zinc were studied. The nanoparticles were characterized by dynamic light scattering, zeta potential and pH measurements. The results showed that an increase in the ionic strength of the solvent provided nanoparticles with considerably narrower size distributions compared to pure water, and a small size. The zinc content was shown to be an important factor for the formation of the nanoparticles. In fact, a critical zinc concentration was needed to obtain nanoparticles, and below this concentration particles were not formed. A stepwise increase in the amount of zinc revealed the process of formation of the nanoparticles. The stages of the nanoparticle formation process were identified, and differences according to the ionic strength of the solvent were also reported. Furthermore, the stability test of the most promising formulation showed a stability of over ten weeks.

Introduction

Polymeric nanoparticles are gaining an increased interest in pharmaceutical applications, in particular in the drug delivery field.¹⁻⁵ In fact, the encapsulation of a drug in polymeric nanoparticles can provide important advantages, such as modification of the drug release profile,⁶ targeting,^{7,8} reduction of the drug degradation,⁹ or bioadhesion.¹⁰ Therefore, the employment of polymeric nanoparticles as drug carriers could provide, for example, an improvement of bioavailability, dose reduction, reduction of the frequency of administration, increased stability, and reduction of the side effects of the drug. Between all the polymers employed for the production of nanoparticles, polysaccharides are of particular interest, especially in virtue of their biocompatibility and biodegradability. For example; pectin,¹¹ chitosan,¹² and alginate¹³ are promising natural polysaccharides used for the preparation of nanoparticles. In addition to their carrier function, polysaccharide-based nanoparticles could also provide therapeutical effects depending on the type of polysaccharide that constitutes them. In fact, unloaded nanoparticles made of chitosan and alginate have demonstrated both antibacterial and anti-inflammatory effect.¹⁴ Moreover, previous studies¹⁵ have shown that alginate can exert an anti-oxidant effect.

Alginate is a natural polysaccharide derived from seaweed, and is already used as a thickening agent in food industry, as well as

in many cosmetic and pharmaceutical products, due to lack of toxicity¹⁶ and low cost. Alginate's most exploited characteristic in drug formulation is the gel forming property, since, in this form, alginate is bioadhesive and the drug release can be controlled.¹⁷⁻¹⁹

Alginate is a linear polymer formed by negatively charged blocks of *D*-mannuronic acid (M) and *L*-guluronic acid (G), separated by single units of M and G. Alginate's negative charged residues can form ionic bonds with divalent cations, which act as cross-linkers between different alginate chains. In this way an ionotropic gel formation occurs.²⁰ The most common cross-linker investigated for alginate is calcium, but other cations can also be employed.^{21, 22} Different types of alginate contain different percentages of M and G. G shows more affinity to divalent cations compared to M, so the types of alginate that contain a higher G percentage lead to the formation of stronger gels, compared to the types of alginate with a higher content of M.²³ The cross-linking mechanism is described as the "egg-box model", where the divalent cations complexate with G or M monomers in an egg-box shape^{17, 24} (Figure 1).

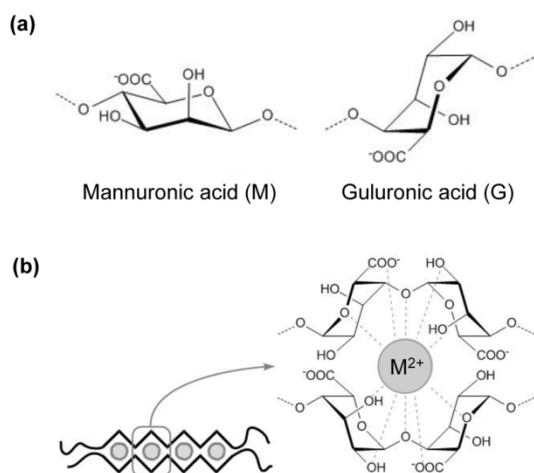


Figure 1. (a) Structure of the alginate monomers: D-mannuronic acid (left) and L-guluronic acid (right). (b) Egg-box structure of the cross-linking between a divalent cation and G monomers of two different alginate chains.

During the gelation process, the cross-linking between overlapped polymer chains forms a macroscopic gel. Nanoparticles are created, instead of gels, when the alginate concentration is lower than the overlap concentration.^{11, 26, 27} Consequently, a local gelation of discrete coils of polymeric chains is promoted.

The most studied nanoparticles prepared by ionotropic gelation are the chitosan-tripolyphosphate (TPP) nanoparticles,^{12, 28-31} while fewer investigations are focused on alginate nanoparticles.³² The alginate nanoparticles have been prepared by alginate-in-oil emulsification method³³ or by self-assembly in an aqueous solvent.^{7, 34} The latter method in particular is interesting for the entrapment of sensitive molecules due to the mild preparation conditions and the avoided use of organic solvents.

The preparation of alginate nanoparticles by self-assembly generally involves a double cross-linking in two steps with a divalent cation (calcium) and a polycation (poly-L-lysine or chitosan).²³ The double cross-linking is necessary since calcium tends to produce colloiddally unstable nanoparticles due to coagulation.^{23, 35} In some studies³⁶ the particles have also been prepared by single cross-linking with the polycation chitosan. However, a formulation with only a divalent cation as the cross-linker could be advantageous. In addition to provide a less laborious one-step preparation compared to the double cross-linking, it allows to avoid the presence of the polycation. In fact, poly-L-lysine can cause immunogenicity and toxicity.³⁷ The possibility of obtaining stable nanoparticles is difficult to predict, and it must usually be determined empirically by varying several variables that can influence the nanoparticle formation.^{23, 34, 38} When chitosan is used as the cross-linker, the number of such variables is increased and this might further complicate the process of formulation. For example, the degree of deacetylation, the molecular weight and the pH of the polymeric solutions also need to be kept in consideration to ensure effective complexation,^{23, 38} and, as a product with

natural origin, the characteristics of chitosan may vary from batch to batch.

This article focuses on the formulation of alginate nanoparticles cross-linked by the single divalent cation zinc. Zinc was chosen as the cross-linker in virtue of its antibacterial properties commonly exploited in formulations for local use³⁹ or oral hygiene.^{40, 41} The aim was to investigate how different important formulation factors affect the ability to produce stable nanoparticles, and to scrutinize the mechanism for the formation of the nanoparticles in order to facilitate future formulation studies. The formulation factors studied were the amount of cross-linker and the presence of monovalent ions in the solvent. The measured characteristics of the nanoparticles were the size distribution, the polydispersity index (PDI), the intensity of scattered light, the zeta potential, and the pH. Atomic force microscopy (AFM) was also employed for the characterization of the samples. Moreover, stability studies of the most promising formulation were carried out over a period of ten weeks.

Materials and Methods

Materials

Sodium alginate (Protanal LF 10/60) was provided by FMC BioPolymer (Norway); the content of G was 65 - 75%, and the content of M was 25 - 35% stated by the manufacturer. Zinc chloride (purity $\geq 98.0\%$) was purchased from Merck (Germany). Sodium chloride (purity 99.9%) was purchased from VWR BDH Prolabo (USA). The water used for the preparation of nanoparticles was purified by a Milli-Q system with 0.22 μm Millipak[®] 40 filter (Millipore[™], Ireland).

Purification and characterization of alginate

Commercially available alginate was dissolved in distilled water (concentration 1.5%, w/w) and stirred overnight at room temperature for complete dissolution. Then, the solution was dialyzed against distilled water in the refrigerator using a Spectra/Por[®] dialysis membrane (Spectrum Laboratoires Inc., CA, USA) with a molecular weight cutoff of 8000 Dalton. The water was changed twice a day for three days, then once a day for additional five days. The dialyzed solution was freeze-dried (Christ Alpha 2-4 freeze drier, Christ, Germany), and the purified and freeze-dried alginate was stored in the refrigerator. The molecular weight was determined by obtaining the intrinsic viscosity $[\eta]$ of the purified alginate in 0.1M NaCl. The measurements were performed by means of a Micro Ostwald capillary viscometer (Schott Geräte, Germany). The semi-empirical Huggins equation was applied to obtain the $[\eta]$ value. Six samples with alginate concentrations ranging from 0.20 to 0.02 g/dl were measured at a constant temperature of 25.0°C, obtaining a good linearity. The relation between $[\eta]$ of the polymer and its viscosity average molecular weight (M_v) is described by the Mark-Houwink equation: $[\eta] = KM_v^\alpha$ where K and α are empiric constants depending on the solvent, the polymer, and the temperature employed during the analysis. K

and α values were previously reported²⁷ as 6.9×10^{-6} and 1.13 respectively for alginate with high G content in 0.1M NaCl at 25°C. By the use of these values, the calculated viscosity average molecular weight of the purified alginate was 147 kDa.

Preparation of the nanoparticles

Alginate nanoparticles were prepared by ionotropic gelation at room temperature, using the cation zinc as the cross-linker. The same method for polymeric nanoparticles preparation was previously reported by others.¹²

Briefly, a solution of alginate and a solution of zinc (chloride) were prepared separately using the same solvent (either Milli-Q water or 0.05M NaCl), and then filtered respectively with 0.80 μ m Millex@AA and 0.22 μ m Millex@GV syringe filters (MilliporeTM, Ireland) in order to avoid dust contamination. Afterwards, 15g of zinc solution were dripped into 60g of alginate solution under constant magnetic stirring (cylindrical stirring bar 6 mm \times 20 mm) at 600 rpm, inside a 100 ml vial (5 cm diameter). A peristaltic pump was employed for the addition of the zinc solution, in order to have a constant and reproducible flow (9.3 ml/min). All other preparation parameters, such as the size, material, and type of the various equipment involved in the preparation, were kept constant. The samples were stirred for ten minutes. Subsequently, the samples were stored overnight at room temperature, and then characterized.

Characterization of the nanoparticles

DYNAMIC LIGHT SCATTERING (DLS). DLS measurements were performed on a Zetasizer Nano ZS (Malvern Instruments Ltd., UK). The samples in polystyrene disposable cuvettes were irradiated with red light laser ($\lambda = 633\text{nm}$), and all the measurements were performed at 25°C with backscatter detection at a scattering angle of 173°. The refractive index and viscosity of pure water at 25°C were used in the calculations as constant parameters, independently of the salinity of the solvent employed. An autocorrelation function was obtained by the intensity fluctuations of the scattered light. The Zetasizer Software (version 6.20) fitted the autocorrelation function with the general purpose fitting method and used the Stokes-Einstein equation to calculate the hydrodynamic diameters of the particles. The data provided by the software were the mean sizes and the polydispersity index value (PDI), together with the intensity-based and volume-based size distribution plots. In addition, the intensity of the scattered light for each sample was also obtained by the measurement of the derived count rate, which corresponds to the number of photons detected per second at the maximum laser power. The results for each sample were obtained as the average of three measurements on the same sample aliquot.

ZETA POTENTIAL. The zeta potential was measured by laser Doppler electrophoresis technique at 25°C using a Zetasizer Nano ZS (Malvern Instruments Ltd., UK). The instrument determines the electrophoretic mobility (U) of the particles when an electric field is applied through laser Doppler velocimetry. The zeta potential (ζ) is calculated from such

measurement on the basis of the Smoluchowski approximation for Henry equation as follows: $U = \epsilon\zeta/\eta$, where the constants ϵ and η are respectively the dielectric constant and the viscosity of the solvent at the analysis temperature. The values of η and ϵ for pure water at 25°C were used in all the measurements (independently of the salinity of the solvent employed). The results for each sample were obtained as the average of five measurements on the same sample aliquot.

pH. The pH of each sample was measured at room temperature with a 744 Metrohm pH meter (Metrohm, Switzerland) calibrated between pH 4 and 7.

Atomic force microscopy (AFM) imaging

AFM imaging was performed using a NanoWizard@ AFM system (JPK Instruments AG, Germany) with NSC35/AIBS Ultrasharp Silicon Cantilevers (MicroMasch, Spain) through intermittent contact mode. The system was set up on an Eclipse TE2000-S inverted optical microscope (Nikon Instruments Inc., Japan) mounted on an anti-vibration table (Halcyonics MOD-1 M plus, Accurion GmbH, Germany).

Three samples were selected for AFM imaging. For each sample, 10 μ l of suspension were placed onto freshly cleaved mica. The suspension in excess was wiped away with a filter paper after allowing three minutes for adsorption. Each slide was rinsed four times with 10 μ l of Milli-Q water, and the slides were allowed to dry overnight at room temperature. AFM imaging was performed the following day after the preparation of the sample.

Experimental design

The influence of the zinc to alginate ratio on the nanoparticles characteristics and the influence of the ionic strength of the solvent were investigated, while the alginate concentration was kept constant at 0.05% (w/w). The ratios between zinc and alginate are expressed as weight to weight (w:w) ratios. Twelve different combinations were prepared. The factors and the levels for the study are listed in Table 1. The three samples selected for AFM imaging were prepared with 0.05% alginate and ratios between zinc and alginate of 0:100, 25:75 and 35:65.

Table 1. Factors and levels in the experimental design.

Factors	Experimental levels
Type of solvent	Water, 0.05M NaCl
Alginate concentration ^a (% w/w)	0.05
Ratio ^b (zinc : alginate)	0:100, 20:80, 25:75, 30:70, 35:65, 40:60

^a Concentration in the final preparation.

^b Expressed as weight to weight (w:w) ratio.

The stability of the samples composed of 0.05% alginate and 35:65 zinc to alginate ratio in 0.05M NaCl was also

investigated. The particles were stored in refrigerator and were characterized one week, four weeks, and ten weeks after preparation.

At least three parallel batches were prepared for each combination in the whole study.

Results

The size distributions for all the experiments in 0.05M NaCl can be found in figure 2. The size distributions are reported instead of mean size values, since the size distributions were broad and multimodal, therefore the mean size values could not be estimated correctly.^{42, 43} Both the size distributions against the intensity of the scattered light and against the volume occupied by the particles are given (figure 2a and 2b, respectively). The volume plots show two shifts of the main peak toward larger sizes when the zinc content was increased. The first slight shift occurred at a zinc to alginate ratio of 25:75. At 35:65 a second important shift occurred from tens to hundreds of nanometers. The intensity plots show clearly that the size distributions were multimodal for most of the formulations. However, when the zinc amount was increased, the broadness of the intensity-based size distributions decreased until a monomodal size distribution was obtained at zinc to alginate ratios of 35:65 and 40:60. For these two combinations the intensity plots were relatively well overlapped with the volume plots. The average hydrodynamic diameters (z-average) for the monomodal distributions were 200nm at zinc to alginate ratio of 35:65, and 230nm at 40:60.

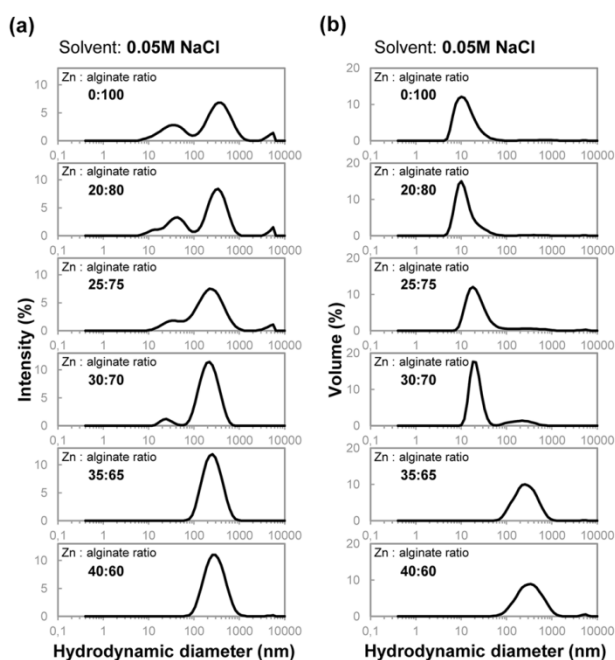


Figure 2. (a) The intensity-based and (b) the volume-based size distributions of the samples with 0.05% alginate prepared in 0.05M NaCl. The curves shown are the average curves of the sample repetitions.

As a consequence of the reduction of the broadness of the intensity-based size distribution, the PDI values also decreased

when the zinc concentration was increased (figure 3a). The minimum PDI value (0.28) was reached at a zinc to alginate ratio of 35:65 in 0.05M NaCl. Hence, the PDI and the size distribution in 0.05M NaCl were shown to be highly dependent on the amount of zinc.

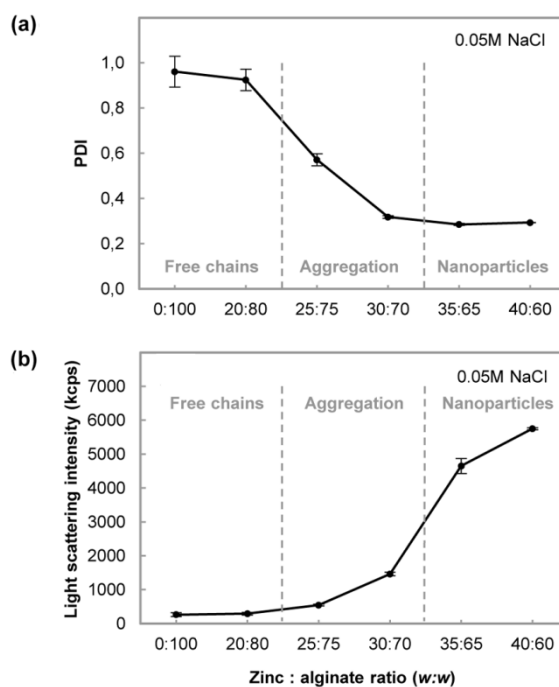


Figure 3. (a) The PDI and (b) the intensity of the scattered light of the samples prepared with 0.05% alginate in 0.05M NaCl. The error bars are standard deviations, and the points without error bars have standard deviations equal or smaller than the size of the symbols. The lines between the symbols are guides to the eye.

The intensity of the scattered light was also dependent on the zinc content, in fact, when increasing the amount of zinc, the scattered intensity was also increasing (figure 3b). The graph of the intensity of the scattered light plotted against the zinc to alginate ratio shows a sigmoidal shape, and the steep increase in the scattered intensity was recorded at zinc to alginate ratio of 35:65. This point corresponds to the minimum PDI value (figure 3a) and to the monomodal size distribution (figure 2a and 2b). Three zones can be identified in the graphs in figure 3. In the first zone, a negligible variation in the PDI and the scattered intensity is observed (free alginate chains); in the second zone, PDI decreases together with the broadness of the intensity-based size distributions, while the scattered intensity grows exponentially (aggregation of the alginate chains); in the third zone, the PDI value remains low and the increase in the scattered intensity is reduced (nanoparticles). When nanoparticle preparation was attempted in water, the characteristics of the aggregates were also dependent on the zinc content. No data are shown for the samples containing a zinc to alginate ratio of 40:60, because flocculation and sedimentation occurred immediately after preparation. Both the intensity-based and the volume-based size distributions were

multimodal for all the samples prepared in water (figure 4a and 4b, respectively).

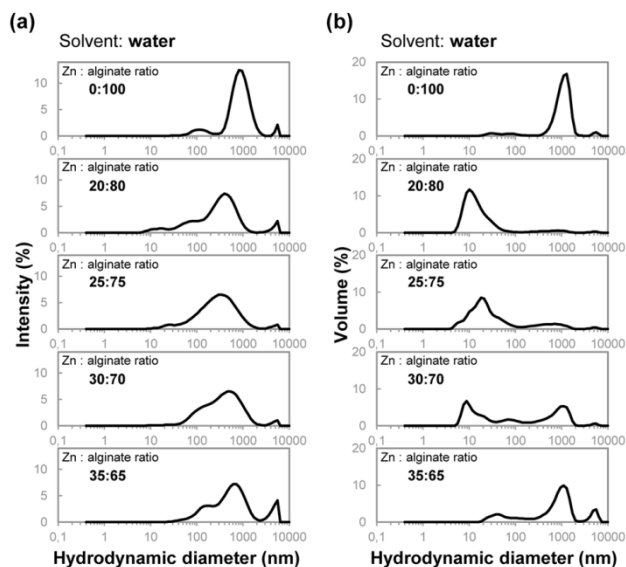


Figure 4. (a) The intensity-based and (b) the volume-based size distribution plots of the samples with 0.05% alginate prepared in water. The curves shown are the average curves of the sample repetitions.

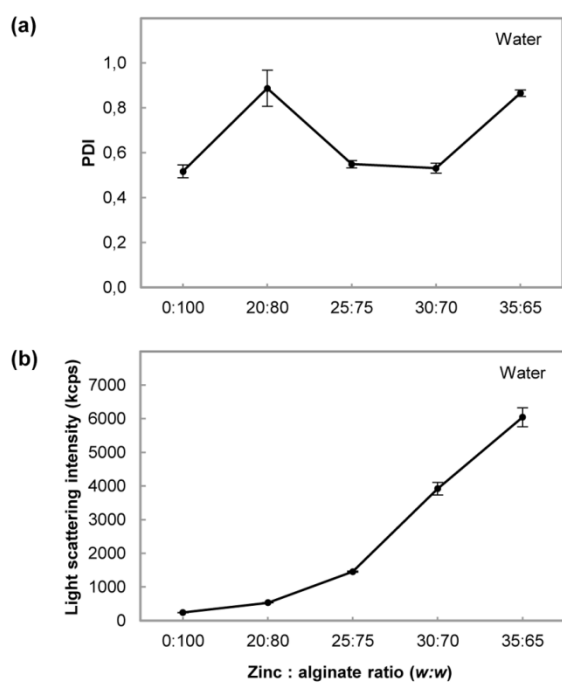


Figure 5. (a) The PDI and (b) the intensity of the scattered light of the samples with 0.05% alginate prepared in water. The sample prepared with a zinc to alginate ratio of 40:60 precipitated immediately after preparation, so no data are shown for that sample. The error bars are standard deviations, and the points without error bars have standard deviations equal or smaller than the size of the symbols. The lines between the symbols are guides to the eye.

The PDI values and the intensity of the scattered light of the samples prepared in water are shown in figure 5. PDI values in the absence of NaCl were consistently high. The apparent PDI value in the absence of zinc (0:100 zinc to alginate ratio) was

0.52, and increased when zinc was added (20:80 zinc to alginate ratio) (figure 5a). When the zinc amount was further progressively increased, the apparent PDI value decreased to a minimum value (0.53) at a zinc to alginate ratio of 30:70, and then it increased again. In the graph of the scattered intensity against the zinc to alginate ratio, the increase in the scattered light seems exponential for zinc to alginate ratios below 25:75 and linear above 25:75 (figure 5b). The steepest increase in the scattered intensity was observed at a zinc to alginate ratio 30:70 where the minimum apparent PDI value was also reached. Such steep increase in the scattered light intensity was also observed at a zinc to alginate ratio of 35:65. The three zones found in the graphs for 0.05M NaCl in figure 3 cannot be clearly defined in water, since in water the different steps may seem to overlap with each other (as further explained in the discussion). Comparing the data obtained in 0.05M NaCl and in water, the minimum apparent PDI value in water was higher than the minimum PDI value in 0.05M NaCl, and occurred at a lower zinc to alginate ratio. In addition, in 0.05M NaCl it was possible to use higher amounts of zinc (40:60 zinc to alginate ratio) and still avoid precipitation.

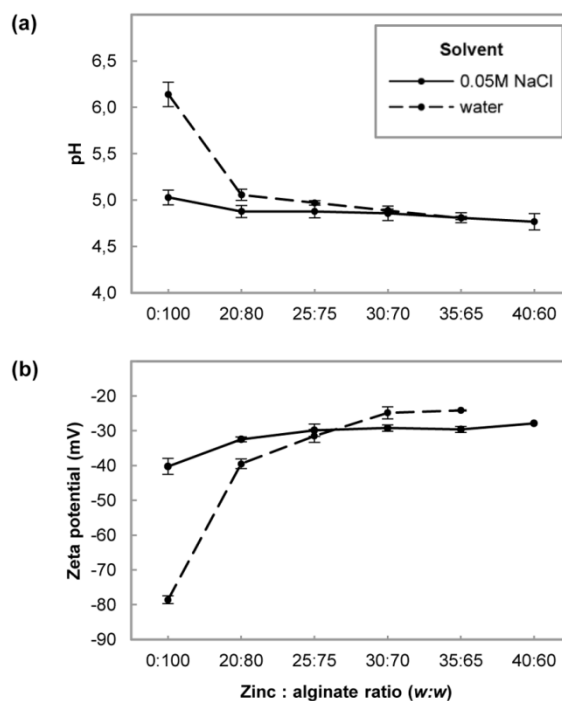


Figure 6. (a) The pH and (b) the zeta potential of the samples prepared with 0.05% alginate in water and in 0.05M NaCl. The error bars are standard deviations, and the points without error bars have standard deviations equal or smaller than the size of the symbols. The lines between the symbols are guides to the eye.

In figure 6 the pH and the zeta potential of the combinations both in water and 0.05M NaCl are shown. The highest pH of 6.1 was obtained for the combination prepared in water without zinc (0:100 zinc to alginate ratio), while the combination without zinc prepared in 0.05M NaCl had a lower pH of 5.0 (figure 6a). In both water and 0.05M NaCl, the pH ranged

between 4.8 and 5.1 in all the samples containing zinc, and the pH slightly decreased when increasing the zinc concentration, since the zinc solutions had a lower pH than the alginate solutions. The zeta potential values were negative for all the formulations, and were strictly related to the pH values (figure 6b); in fact the decrease of the absolute values of the zeta potential was correlated to the decrease in the pH.

The sample composed of 0.05% alginate and a zinc to alginate ratio of 35:65 in 0.05M NaCl was chosen for the stability measurements in virtue of its monomodal size distribution and the lowest PDI value. The particles were stable over a 10 weeks period. The PDI value, the pH, and the zeta potential did not change, the size distributions remained monomodal and no macroscopic flocculation appeared. The only minor variation was a slight increase of 20 nm in the z-average size during the whole 10 weeks period, and the highest size increase appeared during the first week of storage (figure 7). A consequent slight increase proportional to the size increase also occurred in the scattered intensity.

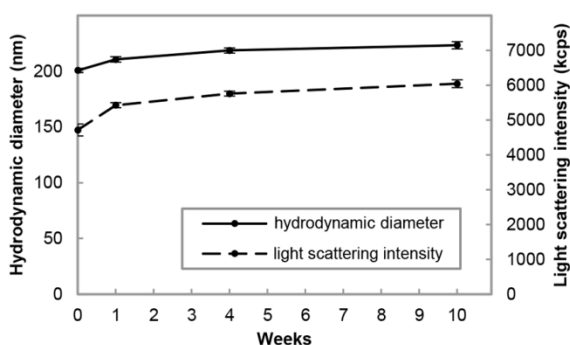


Figure 7. The light scattering intensity and the hydrodynamic diameter (z-average) of the particles composed of 0.05% alginate and a zinc to alginate ratio of 35:65 in 0.05M NaCl measured during a 10 weeks period. The error bars are standard deviations, and the points without error bars have standard deviations equal or smaller than the size of the symbols. The lines between the symbols are guides to the eye.

Discussion

The purpose of this study was to investigate the possibility of preparing stable alginate nanoparticles cross-linked with zinc, and to identify the optimal formulations that provide monomodal size distributions. Additionally, the mechanism of the nanoparticle formation was analysed, since a deeper insight in such process could facilitate future formulation studies.

The pKa value for G and M is around 3.5,⁴⁴ therefore the alginate carboxylic groups were negatively charged in all the samples (pH around 5). This was also confirmed by the negative value of the zeta potential. The presence of negative charges causes repulsion between the alginate chains and allows for binding by the positively charged zinc.

Evaluation of the formation of alginate-zinc nanoparticles in 0.05M NaCl

When evaluating the formation of nanoparticles, the intensity of scattered light can be used to assess the level of chain aggregation and thereby cross-links since the scattered light depends on the size and on the compactness of the aggregates. Previous studies suggested a relation between the particle formation and the intensity of scattered light^{31, 45, 46} or the turbidity²³ during the titration of a cross-linker into a polysaccharide solution. Therefore, by combining the data of light scattering, PDI, and size distribution, it was possible to identify a possible process for the formation of the nanoparticles. Figure 8 illustrates our proposed mechanism for the formation of nanoparticles when the zinc content in the preparation was increased.

When alginate is dissolved in 0.05M NaCl in the absence of zinc or in the presence of small amounts of zinc (20:80 zinc to alginate ratio), the alginate chains are free (stage 1). In fact, the high PDI and the multimodal intensity size distribution showed that no constant sized entities were present, and the extremely low scattered intensity might suggest that no compact aggregates were formed. The very small size shown by the main peak of the volume size distribution could correspond to the apparent size of the free alginate chains. In this stage, the small amount of zinc was not sufficient to provide cross-linking and molecular aggregation. In fact the cross-links formation could possibly be discouraged by the competition between the zinc and the sodium cations in solution.

When the amount of zinc was increased, zinc outdoes the sodium cations and a progressive chain aggregation occurs (stage 2). The mechanism reported for the aggregation of alginate chains due to increasing amount of calcium, has been based on the formation of point-like cross-links due to single calcium cations,⁴⁷ followed by formation of dimers with an egg-box conformation, and eventually the association of the dimers into multimers.⁴⁸ In the present study is not possible to distinguish such steps of chain aggregation, but the formation of cross-links was confirmed by the increase of the scattered intensity, and by the slight shift of the main peak in the volume size distribution plot toward higher sizes compared to the size shown for the free chains (figure 2). Moreover, the progressive decrease of the PDI and of the broadness of the multimodal intensity size distributions indicated the formation of colloidal entities with a more constant size.

The formation of the highest number of cross-links occurred in the sample with a zinc to alginate ratio of 35:65, as suggested by the highest increase in the scattered intensity. Also, a monomodal intensity size distribution was obtained for the first time, and the lowest PDI was recorded, suggesting the formation of relatively constant sized colloidal entities. A further increase in zinc (40:60 zinc to alginate ratio) led to a reduced increase in the scattered intensity, which suggested the formation of a reduced number of cross-links. For this reason, the zinc to alginate ratio of 35:65 could be considered as the point of complete formation of the nanoparticles (stage 3).

Moreover, at this stage, the main peak in the volume-based size distribution plot went through its second shift from tens to hundreds of nanometers. The two peak shifts in the volume plots (the first in stage 2 and the second in stage 3) have previously been observed in a study regarding the preparation of chitosan-TPP nanoparticles.⁴⁵ In that study, the first shift was interpreted as formation of primary aggregates from the chitosan free chains, while the second peak shift was interpreted as the aggregation of the primary aggregates into the final secondary nanoparticles. AFM images in figure 8 seem to confirm that this theory may also be valid for the prepared alginate-zinc nanoparticles. In fact, when comparing the image of the free alginate chains in the absence of zinc (stage 1) and the image of the sample with a zinc to alginate ratio of 25:75 (stage 2), it can be observed in the latter image the possible presence of small primary aggregates together with free unreacted alginate. Moreover, the image of the sample with a zinc to alginate ratio of 35:65 (stage 3) shows the presence of fully formed bigger sized nanoparticles.

The reduced increase in the scattered light has previously^{31, 46} been interpreted as the point of saturation of the intra-particle binding sites of the polymeric chains. Such interpretation can also be applied to our data, where the saturation would occur at a zinc to alginate ratio of 35:65. When the zinc amount was increased beyond the saturation level, the only significant modifications, except a low increase in scattered light, was a slight increase in the apparent mean particle size. The reason could be the formation of a small number of inter-particle cross-linking, probably causing some aggregation between the nanoparticles (stage 4). As speculated in other studies,^{46, 49} these data may suggest that, when zinc is added to the formulation, intra-particle cross-linking occurs preferably, until saturation of the cross-linking sites in the core of the particle; while no cross-linking occurs at the surface of the particle. In

fact, at stage 3 and 4 where the supposed saturation occurred, the zeta potential values were negative, indicating a charged particle surface. After the saturation point, some inter-particle cross-linking occurs on the particle surface, but the aggregation is reduced compared to the previous intra-particle cross-linking. As a previous study⁴⁹ hypothesized, the reason could be the higher difficulty in forming stable bonds on the nanoparticle surface compared to the core, thus the inter-particle bond and the neutralization of the nanoparticles surface due to cross-linking would be discouraged. The difficulty in forming stable bonds on the nanoparticle surface might be due to for example conformational features, such that only few charges are accessible to form stable cross-links.

Evaluation of the formation of alginate-zinc nanoparticles in water

Since both water and 0.05M NaCl were employed as solvents for particle preparation, it was possible to investigate how the presence or absence of monovalent ions could influence the nanoparticle formation.

In water, in the absence of zinc, alginate seemed to form aggregates of relatively constant size. In fact, despite the multimodal size distribution, the apparent PDI was relatively low and the size distribution plots showed the majority of the aggregates sized around 1000nm (figure 4 and 5a). Alginate chains in solution can form clusters,⁵⁰ in fact they can associate for example through hydrogen bonding between the hydroxy groups. The very low level of scattered intensity implies that the aggregates are very swollen. This confirms the weakness of the inter-chains bonds, whose strength is not sufficient to overcome the electrostatic repulsive forces between the chains and to cause the shrinkage of the aggregates.

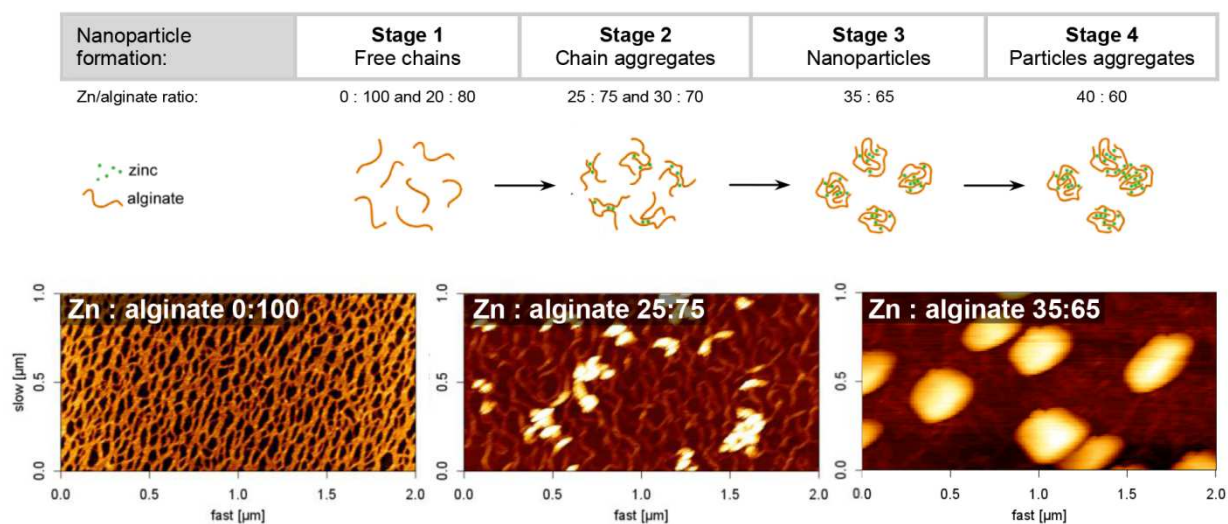


Figure 8. Schematic illustration of the stages of nanoparticle formation. Below, AFM images of samples prepared with 0.05% alginate and a zinc to alginate ratio of 0:100 in water (left), 25:75 (center), and 35:65 (right) in 0.05M NaCl.

When adding a small amount of zinc to the sample (20:80 zinc to alginate ratio), the size distribution became more polydispersed and the big swollen aggregates disappeared. In fact, the interaction between zinc and the charges on the alginate chains probably breaks the weak bonds between the chains, causing disruption of the aggregates. In 0.05M NaCl such swollen aggregates were not formed, probably because NaCl disturbed the formation of the bonds between the alginate chains.

The same stages of nanoparticle formation seemed to find place both in water and in 0.05M NaCl, but in water the distinction between the different stages was not as sharp as in NaCl 0.05M. Cross-linking occurred already at the lowest zinc concentration according to the increase in scattered light, since zinc was not competing with other cations. When the cross-linker concentration was increased, the scattered intensity increased exponentially as in stage 2 in 0.05M NaCl, suggesting an increased aggregation as more zinc was added. The apparent PDI was decreasing, indicating that colloidal entities of more constant size were formed, but monomodal size distributions were never obtained at any of the investigated zinc concentrations. For this reason, it was not possible to distinguish clearly stage 3. Nevertheless, since the highest variation in scattered light and the minimum apparent PDI were obtained at a zinc to alginate ratio of 30:70, it is reasonable to think that at this ratio the highest amount of constant sized aggregates has been formed. In fact, in the volume-based plot a substantial increase in the peak around 1000nm was observed, which could be due to the formation of particles (figure 4). But at the same time, smaller entities in the range 10-100nm and bigger aggregates in the micron range were present, which might be due respectively to partially bound or free alginate chains and to the aggregation of the particles. The simultaneous presence of colloidal entities belonging to all the stages of nanoparticle formation might suggest that in water the stages of nanoparticle formation occur simultaneously.

A further increase in the amount of zinc (35:65 zinc to alginate ratio) caused an increase in the apparent PDI and in the tendency for aggregation. The aggregation is noticeable in the increase of the scattered light, which did not diminish as in 0.05M NaCl, and in the increase of the clusters' peak in the micron range in the size distribution plots. In water ionic bridging between the particles (stage 4) seems to occur to a higher extent than in 0.05M NaCl. In fact, even flocculation and precipitation of a macroscopic gel occurred at 40:60 zinc to alginate ratio, and it could be due to the ionic bridging between particles, which might increase the cluster size and decrease their charge. Therefore, the particles prepared in water showed a considerably lower colloidal stability than the particles prepared in 0.05M NaCl. Aggregation and precipitation were also observed in previous studies when high amounts of cross-linker were added during the preparation of chitosan-TPP nanoparticles in water.^{49, 51}

System modifications induced by the presence of a monovalent salt

When comparing the results of the samples prepared in water and in 0.05M NaCl, it is possible to point out some differences in the two systems, which can be due to the competition between monovalent and divalent ions for the binding site on the polyelectrolyte.⁴⁹

The transitions between the different stages of the nanoparticle formation at increasing zinc concentrations seemed to occur at lower zinc to alginate ratios when the sample was prepared in water compared to the samples prepared in 0.05M NaCl. The reason could be that a higher concentration of zinc may be needed in 0.05M NaCl to form the same number of cross-linking bonds formed in water, since sodium tends to compete with zinc for the binding sites on alginate.

In water the broadness of the size distributions and the PDI values tended to be higher than in 0.05M NaCl. This is in agreement with a previous study,⁴⁹ where the presence of NaCl was shown to decrease the speed of formation of the cross-linking bond due to the ionic competition with the monovalent salt. During the sample preparation, a zone with a high zinc concentration was present for a short time after the addition of zinc. In the presence of NaCl, the mixing could distribute the zinc uniformly throughout the whole sample, allowing for a homogeneous distribution of zinc before the alginate-zinc bond was formed. However, in water the alginate-zinc binding occurred fast, so the inhomogeneous distribution of the cross-linking bonds may cause the simultaneous presence of colloidal entities belonging to different stages of the nanoparticle formation, which explains the high PDI and the multimodal size distributions.

When zinc was employed in excess after nanoparticle formation (stage 4), in 0.05M NaCl the system remained stable and only a slight increase in the size and the PDI was observed, while in water aggregation occurred, until macroscopic flocculation and precipitation appeared. As previously explained for chitosan-TPP systems which showed the same behavior,⁴⁹ NaCl increases the stabilization against nanoparticle aggregation, probably due to the reduced strength of the alginate-zinc bond resulting from the zinc-sodium competition. In this way, the inter-particle bridging that causes aggregation and precipitation could be discouraged.

Storage stability

Alginate nanoparticles have previously been reported to be colloidally unstable when prepared through a simple divalent cation cross-linking, due to the immediate aggregation caused by the formation of cation bridges between the particles.^{30, 34} As shown in our experiments, the addition of NaCl not only prevented the aggregation occurring during the nanoparticle preparation, but allowed for a long term stability over a two weeks period.

A slight increase in the particle size was recorded during the first week of storage, suggesting that the complete equilibration of the system was reached one week after preparation (figure

7). A size increase during the first week after preparation has been also recorded previously for chitosan-TPP nanoparticles⁴⁵ and it was then interpreted as the time needed for the complete formation of the particles.

Conclusions

Stable alginate nanoparticles were successfully prepared through cross-linking with the single divalent cation zinc by increasing the ionic strength of the solvent (0.05M NaCl). Consequently, through the addition of sodium chloride the use of polycations may be not needed in order to obtain stable nanoparticles.^{23, 35} The developed one-step method of preparation at mild conditions is simple and time saving, with no need for sonication, pH adjustments or organic solvents. The achieved particle size was small and the size distributions were monomodal and narrow. This is important to assure the same characteristics of the nanoparticles in the whole batch, in order to provide uniform bioavailability, drug release rate, biodistribution and passive targeting.⁵² For this reason small and uniformly sized nanoparticles could be promising as drug carriers, provided their lack of toxicity.

As expected, the zinc content was shown to be an important factor for the formulation of the nanoparticles and allowed to identify the nanoparticle formation process. A general mechanism of formation for polysaccharide nanoparticles during ionic cross-linking has not yet been defined. Nevertheless, the formation of primary aggregates followed by merging into secondary nanoparticles was previously observed in a study regarding positively charged chitosan-TPP nanoparticles.⁴⁵ The observation of the same mechanism of particle formation for the negatively charged alginate-zinc nanoparticles in this study could possibly confirm the generality of such mechanism.

In conclusion, the high storage stability of over ten weeks of the alginate nanoparticles could allow avoiding further processing of the samples, such as lyophilization,⁵³ which is usually suggested for polymeric nanoparticles. Therefore, alginate-zinc nanoparticles could represent an interesting alternative to the alginate nanoparticles cross-linked with polycations.

Acknowledgements

The authors acknowledge FMC BioPolymer for kindly donating the alginate.

Notes and references

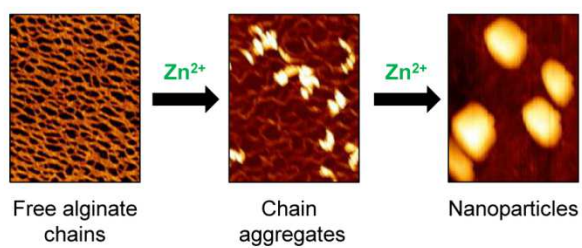
SiteDel Group, School of Pharmacy, University of Oslo, Norway.

* sara.pistone@farmasi.uio.no

- L. M. Ensign, R. Cone and J. Hanes, *J. Controlled Release*, 2014, **190**, 500-514.
- M. M. Mehanna, S. M. Mohyeldin and N. A. Elgindy, *J. Controlled Release*, 2014, **187**, 183-197.
- H. Y. Cho and Y. B. Lee, *J. Nanosci. Nanotechnol.*, 2014, **14**, 868-880.
- A. Dominguez, B. Suarez-Merino and F. Goni-de-Cerio, *J. Nanosci. Nanotechnol.*, 2014, **14**, 766-779.
- E. Gundogdu and A. Yurdasiper, *Int. J. Endocrinol. Metab.*, 2014, DOI: 10.5812/ijem.8984.
- Z. Ahmad, S. Sharma and G. K. Khuller, *Int. J. Antimicrob. Agents*, 2005, **26**, 298-303.
- B. Sarmento, A. Ribeiro, F. Veiga, P. Sampaio, R. Neufeld and D. Ferreira, *Pharm. Res.*, 2007, **24**, 2198-2206.
- P. Verderio, L. Pandolfi, S. Mazzucchelli, M. R. Marinuzzi, R. Vanna, F. Gramatica, F. Corsi, M. Colombo, C. Morasso and D. Prosperi, *Mol. Pharmaceutics*, 2014, **11**, 2864-2875.
- C. P. Reis, A. J. Ribeiro, S. Houg, F. Veiga and R. J. Neufeld, *Eur. J. Pharm. Sci.*, 2007, **30**, 392-397.
- L. M. Ensign, B. C. Tang, Y. Y. Wang, T. A. Tse, T. Hoen, R. Cone and J. Hanes, *Sci. Transl. Med.*, 2012, DOI: 10.1126/scitranslmed.3003453.
- H. Jonassen, A. Treves, A. L. Kjoniksen, G. Smistad and M. Hiorth, *Biomacromolecules*, 2013, **14**, 3523-3531.
- H. Jonassen, A. L. Kjoniksen and M. Hiorth, *Colloid Polym. Sci.*, 2012, **290**, 919-929.
- A. H. Machado, D. Lundberg, A. J. Ribeiro, F. J. Veiga, B. Lindm and M. G. Miguel and U. Olsson, *Langmuir.*, 2012, **28**, 4131-4141.
- A. J. Friedman, J. Phan, D. O. Schairer, J. Champer, M. Qin, A. Pirouz, K. Blecher-Paz, A. Oren, P. T. Liu, R. L. Modlin and J. Kim, *J. Invest. Dermatol.*, 2013, **133**, 1231-1239.
- M. Sen, *Appl. Radiat. Isot.*, 2011, **69**, 126-129.
- T. A. Becker, D. R. Kipke and T. Brandon, *J. Biomed. Mater. Res.*, 2001, **54**, 76-86.
- H. H. Tønnesen and J. Karlsen, *Drug Dev. Ind. Pharm.*, 2002, **28**, 621-630.
- F. Sevgi, B. Kaynarsoy, M. Ozyazici, C. Pekcetin and D. Ozyurt, *Pharm. Dev. Technol.*, 2008, **13**, 387-392.
- N. Salamat-Miller, M. Chittchang and T. P. Johnston, *Adv. Drug Delivery Rev.*, 2005, **57**, 1666-1691.
- D. Hudson and A. Margaritis, *Crit. Rev. Biotechnol.*, 2013, **34**, 161-179.
- A. Haug and O. Smisrød, *Acta Chem. Scand.*, 1970, **24**, 843 - 854.
- Y. A. Morch, I. Donati, B. L. Strand and G. Skjak-Bræk, *Biomacromolecules*, 2006, **7**, 1471-1480.
- S. De and D. Robinson, *J. Controlled Release*, 2003, **89**, 101-112.
- S. N. Pawar and K. J. Edgar, *Biomaterials*, 2012, **33**, 3279-3305.
- G. T. Grant, E. R. Morris, D. A. Rees, P. J. C. Smith and D. Thom, *FEBS Lett.*, 1973, **32**, 195-198.
- M. T. Nickerson and A. T. Paulson, *Carbohydr. Polym.*, 2004, **56**, 15-24.
- A. Martinsen, G. Skjåk-Bræk, O. Smidsrød, F. Zanetti and S. Paoletti, *Carbohydr. Polym.*, 1991, **15**, 171-193.
- Q. Gan, T. Wang, C. Cochrane and P. McCarron, *Colloids Surf.*, 2005, **44**, 65-73.
- T. Lopez-Leon, E. L. Carvalho, B. Seijo, J. L. Ortega-Vinuesa and D. Bastos-Gonzalez, *J. Colloid Interface Sci.*, 2005, **283**, 344-351.
- Y. Lapitsky, *Curr. Opin. Colloid Interface Sci.*, 2014, **19**, 122-130.
- Y. Cai and Y. Lapitsky, *Colloids Surf., B*, 2014, **115**, 100-108.
- J. P. Paques, E. van der Linden, C. J. van Rijn and L. M. Sagis, *Adv. Colloid Interface Sci.*, 2014, **209**, 163-171.
- J. O. You and C. A. Peng, *Macromol. Symp.*, 2005, **219**, 147-153.

34. M. Rajaonarivony, C. Vauthier, G. Couarraze, F. Puisieux and P. Couvreur, *J. Pharm. Sci.*, 1993, **82**, 912-917.
35. B. Sarmiento, A. J. Ribeiro, F. Veiga, D. C. Ferreira and R. J. Neufeld, *J. Nanosci. Nanotechnol.*, 2007, **7**, 2833-2841.
36. S. K. Motwani, S. Chopra, S. Talegaonkar, K. Kohli, F. J. Ahmad and R. K. Khar, *Eur. J. Pharm. Biopharm.*, 2008, **68**, 513-525.
37. B. L. Strand, L. Ryan, P. I. Veld, B. Kulseng, A. M. Rokstad, G. Skjåk-Bræk and T. Espevik, *Cell Transplantation*, 2001, **10**, 263-275.
38. K. L. Douglas and M. Tabrizian, *J. Biomater. Sci., Polym. Ed.*, 2005, **16**, 43-56.
39. M. C. Straccia, G. G. d'Ayala, I. Romano and P. Laurienzo, *Carbohydr. Polym.*, 2015, **125**, 103-112.
40. D. Cummins and J. E. Creeth, *J. Dent. Res.*, 1992, **71**, 1439-1449.
41. M. Sanz, J. Serrano, M. Iniesta, I. Santa Cruz and D. Herrera, *Monogr. Oral Sci.*, 2013, **23**, 27-44.
42. U. Nobbmann and A. Morfesis, *MRS Online Proc. Libr.*, 2008, DOI: 10.1557/PROC-1074-11510-1545.
43. U. Nobbmann and A. Morfesis, *Mater. Today* 2009, **12**, 52-54.
44. K. I. Draget, G. Skjåk Bræk and O. Smidsrød, *Carbohydr. Polym.*, 1994, **25**, 31-38.
45. Y. Huang and Y. Lapitsky, *Biomacromolecules*, 2012, **13**, 3868-3876.
46. Y. Huang and Y. Lapitsky, *J. Phys. Chem. B*, 2013, **117**, 9548-9557.
47. M. Borgogna, G. Skjåk-Bræk, S. Paoletti and I. Donati, *J. Phys. Chem. B* 2013, **117**, 7277-7282.
48. Y. Fang, S. Al-Assaf, G. O. Phillips, K. Nishinari, T. Funami, P. A. Williams and L. Li, *J. Phys. Chem. B*, 2007, **111**, 2456-2462.
49. Y. Huang and Y. Lapitsky, *Langmuir*, 2011, **27**, 10392-10399.
50. M. G. Carneiro-da-Cunha, M. A. Cerqueira, B. W. S. Souza, J. A. Teixeira and A. A. Vicente, *Carbohydr. Polym.*, 2011, **85**, 522-528.
51. P. Calvo, C. Remuñán-López, J. L. Vila-Jato and M. J. Alonso, *J. Appl. Polym. Sci.*, 1997, **63**, 125-132.
52. I. Aynie, C. Vauthier, H. Chacun, E. Fattal and P. Couvreur, *Antisense Nucleic Acid Drug Dev.*, 1999, **9**, 301-312.
53. W. Abdelwahed, G. Degobert, S. Stainmesse and H. Fessi, *Adv. Drug Delivery Rev.*, 2006, **58**, 1688-1713.

GRAPHICAL ABSTRACT



Stable alginate nanoparticles have for the first time been prepared by ionic cross-linking with a divalent cation through a simple one-step method. The mechanism of formation was identified.